

1 **Initial experience of the High-Density Grid catheter in patients undergoing**  
2 **catheter ablation for atrial fibrillation**

3  
4  
5 Nikolaos Papageorgiou<sup>1,2</sup>, Nabeela Karim<sup>1</sup>, James Williams<sup>3</sup>, Jason Garcia<sup>1</sup>, Antonio Creta<sup>1</sup>,  
6 Richard Ang<sup>1</sup>, Neil Srinivasan<sup>1</sup>, Rui Providencia<sup>1,4</sup>, Ross J. Hunter<sup>1</sup>, Mehul Dhinoja<sup>1</sup>,  
7 Vivienne Ezzat<sup>1</sup>, Vinit Sawhney<sup>1</sup>, Adam Dennis<sup>1</sup>, Martin Lowe<sup>1</sup>, Pier D. Lambiase<sup>1,2</sup>,  
8 Anthony WC. Chow<sup>1,5</sup>  
9

10  
11 <sup>1</sup>Electrophysiology Department, Barts Heart Centre, St. Bartholomew's Hospital, London UK

12 <sup>2</sup>Institute of Cardiovascular Science, University College London, London, UK

13 <sup>3</sup>Cardiovascular Department of Abbott, UK, London

14 <sup>4</sup>Institute of Health Informatics, University College London, London, UK

15 <sup>5</sup>Queen Mary University, London, UK  
16  
17

18  
19 **Running title:** HD Grid catheter and atrial fibrillation ablation  
20  
21  
22  
23  
24  
25

26 ***Corresponding author:***

27 Dr Anthony WC. Chow MD FRCP

28 Barts Heart Centre, St. Bartholomew's Hospital

29 West Smithfield, EC1A 7BE

30 London, United Kingdom

31 Email: [anthony.chow1@nhs.net](mailto:anthony.chow1@nhs.net)  
32  
33

34 **Abstract**

35

36 **Purpose:** A significant proportion of patients undergoing catheter ablation for atrial  
37 fibrillation (AF) experience arrhythmia recurrence. This is mostly due to pulmonary vein  
38 reconnection (PVR). Whether mapping using High-Density Wave (HDW) technology is  
39 superior to standard bipolar (SB) configuration at detecting PVR is unknown. We aimed to  
40 evaluate the efficacy of HDW technology compared to SB mapping in identifying PVR.

41 **Methods:** High-Density (HD) multipolar Grid catheters were used to create left atrial  
42 geometries and voltage maps in 36 patients undergoing catheter ablation for AF (either due to  
43 recurrence of an atrial arrhythmia from previous AF ablation, or de novo AF ablation).  
44 Nineteen SB maps were also created and compared. Ablation was performed until pulmonary  
45 vein isolation was achieved.

46 **Results:** Median time of mapping with HDW was 22.3 [IQR: 8.2] minutes. The number of  
47 points collected with HDW ( $13299.6 \pm 1362.8$  vs  $6952.8 \pm 841.9$ ,  $p < 0.001$ ) and used  
48 ( $2337.3 \pm 158.0$  vs  $1727.5 \pm 163.8$ ,  $p < 0.001$ ) was significantly higher compared to SB.  
49 Moreover, HDW was able to identify more sleeves (16 for right and 8 for left veins), where  
50 these were confirmed electrically silent by SB, with significantly increased PVR sleeve size  
51 as identified by HDW ( $p < 0.001$  for both right and left veins). Importantly, with the use of  
52 HDW the ablation strategy changed in 23 patients (64% of targeted veins) with a  
53 significantly increased number of lesions required as compared to SB for right ( $p = 0.005$ ) and  
54 left veins ( $p = 0.003$ ).

55 **Conclusion:** HDW technology is superior to SB in detecting pulmonary vein reconnections.  
56 This could potentially result into a significant change in ablation strategy and possibly to  
57 increased success rate following pulmonary vein isolation.

58

59

60 **Keywords:** atrial fibrillation; catheter ablation; pulmonary veins; electrograms

61

62

63

64

65

66

67

68

69

70

71

72

73

74

75

76

77

78

79 **Introduction**

80 Recurrence of atrial fibrillation (AF) following catheter ablation procedures remains an  
81 important clinical problem, with reported rates of 24-55% [1,2] and pulmonary vein  
82 reconnection (PVR) being the most common reason for low success rates of treatment [3,4].  
83 The causes of PVR appear to be multifactorial, with limitations in mapping to identify  
84 substrates for ablation being a major reason.

85 Improvement in mapping to identify pulmonary vein (PV) sleeves and effectiveness of  
86 complete pulmonary vein isolation (PVI) could be the key to prevent AF recurrence. This is  
87 currently achieved with incremental procedures [5], improved ablation techniques [6-9]  
88 confirming bidirectional block [10], prolonged waiting times after PVI, uncovering dormant  
89 PVR with agents such as adenosine [11]. Improvements in mapping technology may lead to  
90 higher freedom from AF [1]. Despite promising advances made in PVI techniques, PVR still  
91 rates remain high. The concept of manipulating wavefront directionality to map PV ostia for  
92 isolation has not been utilized independently to identify PVR.

93 The High-Density (HD) Grid catheter consists of 16 electrodes mounted on four-splines  
94 within a closed frame (**Figure 1**). The HD Grid mapping catheter has 4 splines, each with 4  
95 small (1 mm) equally spaced (3 mm) electrodes. Unlike standard multipolar mapping, the HD  
96 Grid is the only available system that enables simultaneous assessment of both adjacent and  
97 orthogonal electrograms (EGMs). The spline electrodes are thin, fixed but highly flexible,  
98 mounted on a bi-directional deflectable catheter. The High-Density Wave (HDW) algorithm  
99 enables EGM data acquisition to be less direction-dependent to create voltage maps. It  
100 automatically selects the EGM with the largest peak-to-peak voltage, comparing orthogonal  
101 planes of activation, whereas standard bipolar (SB) mapping uses a single direction spline  
102 bipoles. This has the distinct advantage of detecting larger EGM signals, independent of  
103 electrode orientation to wavefront direction, as shown in previous experimental studies [12].

104 In the present study, we aim to evaluate the efficacy of HDW technology in identifying PVR  
105 compared to SB mapping in PVI procedures.

106

## 107 **Methods**

### 108 *Study population*

109 36 consecutive patients undergoing AF catheter ablation for PV isolation with the HD Grid  
110 catheter (either due to recurrence of an atrial arrhythmia from previous AF ablation, or de  
111 novo AF ablation) were recruited at Barts Heart Centre, London, United Kingdom, between  
112 December 2017 and November 2019.

113 Patients without PVR were excluded from the study. Each patient acted as their own control  
114 due to the HDW electroanatomical map and SB electroanatomical map being taken  
115 simultaneously. The study was approved by the local Hospital Ethics Committee. Patients  
116 gave written informed consent.

117

### 118 *Procedural characteristics*

119 All procedures were performed under conscious sedation or general anesthesia. Right femoral  
120 venous access was obtained using ultrasound guidance in all cases. A decapolar catheter (6F  
121 Cournand fixed curve, Boston Scientific) was placed in the coronary sinus for pacing  
122 maneuvers and used as reference for electroanatomical mapping and activation timings.  
123 Single or double trans-septal puncture was performed with a 71cm Brockenbrough needle  
124 under fluoroscopy guidance or under transoesophageal echocardiogram guidance where  
125 general anesthesia was used. The HD Grid and TactiCath™ (Abbott) irrigated ablation  
126 catheter were introduced into the left atrium through a non-steerable sheath (8.5F SL0 or  
127 SL1, Abbott) and a steerable sheath (Agilis; Abbott). Unfractionated Heparin was given to  
128 maintain activation clotting time above 300 throughout the procedure.

129

130 *Creation of left atrial HDW map*

131 Left atrial (LA) geometry and voltage maps were created using the HD Grid catheter and  
132 EnSite Precision mapping system (Abbott) both in sinus rhythm and in atrial fibrillation  
133 (**Figure 2**). Myocardial voltages  $<0.07\text{mV}$  were considered to be scar and voltages  $>0.5\text{mV}$   
134 were considered to be healthy active myocardium. Voltages between  $0.07\text{-}0.5$  were still  
135 considered to be low, but corresponding to viable tissue, as seen in many patients with  
136 diseased atrium.

137 The HDW algorithm selects the largest peak to peak voltage EGMs obtained from adjacent  
138 orthogonally orientated electrode pairs acquired simultaneously, automatically assigning the  
139 largest detected EGM as activation points to create high density voltage map. Sufficient  
140 points coverage of the entire LA was collected and in particular higher density points were  
141 taken around each PV ostium.

142

143 *Identification of pulmonary vein reconnections*

144 Left atrial voltage maps completed with the HDW were used to guide ablation. Signals were  
145 annotated to the peak deflection (on local EGM) using a EGM voltage  $>0.07\text{mV}$ , while scar  
146 was denoted for voltages  $<0.07\text{mV}$ . Threshold of  $0.07$  threshold was used for both catheters  
147 of the study (HD Grid and SB). A PVR was denoted where there was detectable voltage  
148 above threshold and channels of sequential activation proceeding from the atrium into the  
149 vein confirmed. The number of PVRs which were measured, were identified as distinct  
150 channels surrounded by electrically silent tissue (scar). Activation points were re-annotated to  
151 exclude far-field signals. Differential pacing was utilized, if there was uncertainty of local or  
152 far-field signals. Following completion of the procedure, the number of PVRs were recorded  
153 for each vein as well as the maximal width of each PVR. The presence of PVR was re-

154 confirmed by a second blinded experienced electrophysiologist and cardiac physiologist, who  
155 were blinded to each other's assessment.

156

157 *Radiofrequency ablation*

158 PVR sleeves were targeted for ablation using a force sensing TactiCath catheter, aiming for  
159 10-40g contact. Segmental ablation lesions were delivered at 35-40 Watts energy along the  
160 wide antral circumferential ablation (WACA)/PV ring for the anterior wall and lesions at 30  
161 Watts were delivered on the posterior wall. Energy titration was guided by lesion size index  
162 (LSI), aiming for a target of 4 in the posterior wall and 6 in the anterior wall. The LSI is a  
163 multi-parametric index, which has been validated by both experimental and clinical studies  
164 [13-15], incorporating time, power, contact-force, and impedance data recorded during  
165 radiofrequency ablation in a weighted formula that describes ablation biophysics. Catheter  
166 irrigation was set between 17-30ml/min, depending on power settings used.

167

168 *Confirmation of pulmonary vein isolation*

169 Entry and exit block were assessed in ablated veins and repeat voltage maps were made with  
170 the HD Grid to assess for PVI. As part of the validation protocol for this new catheter, we  
171 aimed to compare the data obtained from a circular mapping catheter (CMC). The choice for  
172 an Optima™ or a Reflexion Spiral™ CMC catheter was left to operator's discretion in order  
173 to confirm PVI after ablation-guided by the HD Grid. This was performed in 53% of patients  
174 with 100% correlation, demonstrating concordance with current practice for PVI.

175

176

177 *Creation of left atrial standard bipolar map*

178 After completion of procedure, the HDW voltage map was converted into a SB map offline  
179 using the TurboMap feature. Unlike to the HDW where the largest peak-to-peak voltage was  
180 automatically selected between adjacent and orthogonal vectors, the SB map was created  
181 from electrogram data taken from a fixed electrode orientation. The same surface points were  
182 used and voltage settings were applied with a range between 0.07-0.5mV for consistency.  
183 AutoMap settings were kept the same for both SB and HDW map for all patients (interior  
184 projection 7mm, exterior projection 7mm and interpolation setting 7) (**Figure 2**). In our  
185 study, PVR was confirmed by a combination of activation and voltage points extending from  
186 the antral chamber leading into the vein, with adjacent electrogram that showed split  
187 potentials of >20msec, considered as a line of block if recorded in sinus rhythm. Pulmonary  
188 vein reconnections were analysed and identified in the same manner as described for the  
189 HDW map. The number of PVRs were recorded by two experienced electrophysiologists and  
190 electrophysiology technicians.

191

192 *Statistical analysis*

193 Descriptive data are presented as numbers and percentages or mean (+/- standard  
194 deviation) or median and inter-quartile range. The Chi-square test was used for comparing  
195 ratios and categorical variables. Comparison of continuous variables was performed using the  
196 paired or unpaired t-test, or their non-parametric equivalents, when appropriate. Results with  
197  $p<0.05$  were considered as significant. PASW Statistics (SPSS Inc, Chicago, IL) version 18.0  
198 was used for statistical analysis.

199

200

201

202 **Results**

203 Thirty-six (36) patients undergoing catheter ablation for PVI were enrolled into our study. Of  
204 these, 33 had previously undergone catheter ablation for paroxysmal/persistent atrial  
205 fibrillation or atrial tachycardia. PVI was performed as part of the procedure in 5 cases of  
206 relevant atrial tachycardia.

207 The mean age of patients was  $66.3\pm 8.1$  years and 39% were female. The mean LA size was  
208  $4.10\pm 0.60$  cm. The median duration of AF history was 38 months. Baseline characteristics of  
209 the patients are presented in **Table 1**.

210

211

212 *Mapping time, points collected and used*

213 Creating detailed maps of the left atrium with the HD Grid required a median of 22.3 [IQR:  
214 8.2] minutes. There was a significant difference between HDW and SB in the number of  
215 points collected and used (**Table 2**). More specifically, the number of points collected and  
216 used with the HDW was significantly higher compared to SB ( $13299.6\pm 1362.8$  vs  
217  $6952.8\pm 841.9$ ,  $p<0.001$  and  $2337.3\pm 158.0$  vs  $1727.5\pm 163.8$   $p<0.001$  respectively) (**Figure**  
218 **S1**).

219

220 *Pulmonary veins: number and size of sleeves*

221 HDW detected 139 PV sleeves, while SB detected 123 PV sleeves (Table 2). HDW was able  
222 to identify 24 sleeves which were not detected by SB mapping. There were a few instances  
223 where SB was better, identifying 9 vein sleeves which were not detected by HDW. In general,  
224 not only were more PVRs identified by HDW compared to SB, but also the ostial width of  
225 reconnections was substantially larger when mapped by HDW compared to SB (right veins:



226 23.0±3.53mm vs 12.7±2.33mm, p<0.001 and left veins: 37.4±6.1mm vs 23.0±5.46mm,  
227 p<0.001), (**Figures 2,3**) (**Table 2**).

228

229 *HD Grid: role in ablation strategy, AF recurrence and safety profile*

230 Allowing for a 5mm ablation lesion size to treat PVR, HDW mapping resulted in a  
231 significantly higher number of lesions for both left (10.9±1.55 vs 7.7±1.13, p=0.005) and right  
232 (8.56±1.16 vs 6.62±1.27, p=0.003) PV applications compared to SB (**Figure 4**), which can  
233 actually be interpreted as a change in ablation strategy in 23 (64%) patients of the study  
234 population.

235 Twenty-nine patients had a minimum of 3months (only one patient, the rest greater than  
236 5months) follow-up. Over a median period of 10 months post-mapping with HD Grid and  
237 ablation, 24 (83%) of the patients remained free of AF. Recurrence of AF was documented in:  
238 1 patient with paroxysmal AF, 2 patients undergoing repeat ablation for paroxysmal AF, 1  
239 patient with persistent AF and 1 patient having repeat ablation for persistent AF.

240 There were 2 cases (5.6%) of acute cardiac tamponade. These were evident during CMC  
241 manipulation, associated with difficulties in CMC navigation causing high forces. Although  
242 both cases were evident whilst using the CMC, a slowly evolving tamponade because of the  
243 previous use of HD Grid cannot be excluded and we therefore do not ascribe both tamponade  
244 cases to CMC. Both cases required pericardial drainage, but no surgical intervention.

245

## 246 **Discussion**

247

248 The cornerstone of AF therapy remains PVI. There has been a number of technological  
249 advances over the last 2 decades, with the aim of achieving complete electrical isolation of  
250 pulmonary veins. These include the development of irrigated ablation catheters, application

251 of higher energies for ablation, use of high resolution mapping and contact-force sensing  
252 catheters. These have achieved single procedure success rates for catheter ablation  
253 procedures generally around 70%. Arrhythmia recurrence post ablation is generally  
254 considered to be due to reconnection of PV sleeves. The current challenge is to develop more  
255 accurate mapping combined with effective ablation therapy, to create more complete and  
256 permanent PVI.

257 There are many variables that affect the resolution of bipolar EGMs including electrode  
258 numbers, spacing and size [16-18]. In this study, wavefront direction technology was used to  
259 independently show its effect on the resolution of bipolar EGMs clinically and therefore alter  
260 the resolution of atrial electroanatomical maps.

261 We have demonstrated that wavefront directionality significantly influences the detection of  
262 PVR. Using HDW technology, orthogonal electrogram processing (2 different orientations of  
263 electrodes-down and across the spline) results in not only more voltage points being taken  
264 and used, but also a significantly higher identification of PVRs compared to SB configuration  
265 (use of electrodes only down the spline-collection only along the longitudinal axis).

266 Previous research has demonstrated that bipolar EGM amplitude is directly affected by  
267 wavefront direction, with the wavefront detection being largest when propagating parallel to  
268 the bipole electrode orientation, and significantly reduced when it is perpendicular to  
269 electrode pair [19,20]. If a wavefront crosses a bipole pair simultaneously, it may show little  
270 or no potential difference. This is of particular importance in PVI procedures, where the end  
271 point of isolation is determined by absence of ostial electrograms recorded by a circular  
272 catheter and this is in turn dependent on the orientation of the catheter electrodes to the  
273 activation wavefront.

274 By its very nature, SB map is limited by its orientation to wavefront progression. This may  
275 lack the sensitivity to detect myocardial sleeves connecting PVs, if paired electrodes are

276 aligned perpendicular to wavefront activation, thus leading some authors to use the term  
277 “bipolar blindness” [21]. In this study, a number of PVs were considered to be silent and  
278 isolated, when in fact clear PVR sleeves were evident when mapped by HDW. In 16 right  
279 and 8 left PVs considered isolated, had clear PVRs. The HD wave algorithm also detected  
280 greater numbers of PVR and the overall width was significantly larger compared to SB  
281 settings, resulting in a change in ablation strategy (delivering more lesions) in 64% of PVRs.  
282 Improving map resolution could increase detection of PVR [16,21] and long term freedom  
283 from atrial arrhythmias [16]. This study using the HD Grid catheter demonstrates the  
284 advantage of improving mapping resolution and how this technology could possibly  
285 overcome the limitations of current SB recordings.  
286 The Grid shape, with thin flexibility splines, can be easily adapted and conformed to complex  
287 PV anatomy and ridges. In fact, the only complication we had was some difficulty in getting  
288 the CMC to sit ostially on small calibre PV, whereas the HD Grid had no problems achieving  
289 mapping nor access. The HD Grid catheter in this study was used by 10 different operators  
290 and was described as easy to manoeuvre by all users.

291

### 292 *Clinical Implications*

293 Recurrence of AF remains a significant challenge in ablation therapy and PVRs are present in  
294 92% of patients undergoing repeat AF ablation procedures [3]. The mechanism responsible  
295 for PVR includes incomplete linear lines leaving anatomic gaps or failure to produce  
296 transmural lesions, leading to PV conduction [22,23]. This study also highlights the complex  
297 role of wavefront direction as well as the limitations of SB mapping. Development of HD  
298 wave technology allows mapping and identifying PVRs with greater resolution. This can  
299 change the ablation strategy and potentially result to improvement in clinical outcomes.

300

301 *Limitations*

302 This is a small pilot study and involves a relatively limited number of patients without a  
303 randomized control arm. Only short term follow up data is available, longer term clinical  
304 outcomes in larger numbers are still awaited to assess the efficacy of HDW mapped for PVI.  
305 It is worth mentioning that not all HD Grid electrodes are always in contact with atrial  
306 tissues, which could potentially affect data acquisition, but this is common across all  
307 commercially available catheters.

308 In the present study, we have recorded the time required for mapping the left atrium with the  
309 HD Grid, however we have not recorded the amount of time used for annotation and analysis.  
310 Each case was not done by the same operator, each case had its own challenges and it was  
311 approached in a different way, while a difficult case would require more time compared to an  
312 easy one. Cases were analysed offline and in retrospect. Again, the same principles applied,  
313 as such it would not be safe/accurate to provide timings and therefore these were not  
314 recorded.

315 Finally, we acknowledge that a CMC should have been used in all our cases, however due to  
316 time and clinical reasons we did not. We tried to avoid extending cases by additional time at  
317 patients' best interest.

318

319 **Conclusions**

320 The simultaneous detection of orthogonal and adjacent EGMs by the HD Grid using HDW  
321 algorithm is significantly superior compared to configuration along spline bipoles at detecting  
322 PVRs. The greater resolution which is achieved by HD Grid, is a promising development in  
323 PVI therapy for AF, but this requires larger scale evaluation.

324

325 **Acknowledgements:** None

326 **Conflict of interest:** Dr Chow receives research grant funding from Abbott and Boston  
327 Scientific Inc.

328  
329  
330  
331

332 **Figure titles & legends**

333

334 **Figure 1. HD Grid catheter design.**

335 Simultaneously adjacent electrograms (EGMs) detect along the Grid splines (in this example  
336 B2-B3) and orthogonal EGMs across Grid spline (in this example B2-C2). HD wave  
337 algorithm selects the largest peak-to-peak voltage obtained from either vector (in this  
338 example B2-C2) and this is assigned as the local EGM at this point on the map. Standard  
339 bipolar algorithm defaults to select EGMs obtained from along the spline bipoles (in this  
340 example B2-B3) regardless of which vector produced the largest peak-to-peak voltage.

341 The HD Grid mapping catheter has 4 splines, each with 4 small (1 mm) equally spaced (3  
342 mm) electrodes. The grid design offers the simultaneous orthogonal bipolar electrogram  
343 recording (along and across the spline).

344

345 **Figure 2. Example of left atrial maps with a right lateral projection of SB data and the  
346 same projection using HDW in AF.**

347 A small anterior right upper pulmonary vein sleeve is seen on the SB map, but a larger more  
348 extensive PVR is detected on the HDW map. The same voltage settings of 0.07-0.5mV were  
349 used to create the maps. The corresponding electrograms around the RUPV are shown on the  
350 right of each map. Much larger and active electrograms are seen with the HDW wave.

351

352 **Figure 3. a) Example of right lower pulmonary vein reconnections mapped during sinus  
353 rhythm.**

354 Comparative maps using HDW on the left are compared to SB on the right. Electrograms  
355 recorded at the RLPV are displayed on each right panel. More extensive reconnections are  
356 seen by the HDW map, with the vein almost totally connected posteriorly, extending into the  
357 inter-venous ridge.

358 **b) Example of voltage maps of the left upper pulmonary (LUPV) comparing standard  
359 bipolar (SB) settings (left panel) compared to HD wave (right panel).**

360 Scar is seen as grey <0.07mV. Sampled electrograms from the circled area are shown on the  
361 panel on the right of each map. Timing markers are seen as single sharp deflections. A CS  
362 reference electrogram is seen at the top in green. The SB map has hardly any electrogram,  
363 whilst the HD wave shows active reconnections leading into the LUPV.

364 **c) Example of left atrial map with roof view projection, created by HDW and SB during  
365 sinus rhythm from LUPV.**

366 Electrograms taken from the left upper pulmonary vein (within the area denoted by the  
367 elliptical black line) are shown on the right of each map. The reference CS electrogram is  
368 shown in green. The left superior pulmonary vein is silent according to the SB map, but the  
369 whole vein is clearly connected on the HDW map, confirmed by the electrograms.

370

371 **Figure 4. Difference in the number of lesions in left and right veins with the use of HD  
372 wave (HDW) and standard bipolar (SB).**

373

374  
375  
376  
377  
378  
379  
380  
381  
382  
383  
384

**Tables**

**Table 1.** Baseline characteristics of the study population

**Table 2.** Procedural characteristics

**Supplementary material**

**Figure S1. Difference in the number of points a) collected and b) used with HD wave (HDW) and standard bipolar (SB).**

385 **References:**

386  
387  
388  
389  
390  
391  
392  
393  
394  
395  
396  
397  
398  
399  
400  
401  
402  
403  
404  
405  
406  
407  
408  
409  
410  
411  
412

1. Nery PB, Belliveau D, Nair GM, et al. Relationship Between Pulmonary Vein Reconnection and Atrial Fibrillation Recurrence: A Systematic Review and Meta-Analysis. *JACC Clin Electrophysiol* 2016; 2: 474–483.
2. Morillo CA, Verma A, Connolly SJ, et al. Radiofrequency ablation vs antiarrhythmic drugs as first-line treatment of paroxysmal atrial fibrillation (RAAFT-2): a randomized trial. *JAMA* 2014; 311: 692–700.
3. Lin D, Santangeli P, Zado ES, et al. Electrophysiologic findings and long-term outcomes in patients undergoing third or more catheter ablation procedures for atrial fibrillation. *J Cardiovasc Electrophysiol* 2015; 26: 371–377.
4. Kuck KH, Hoffmann BA, Ernst S, et al. Impact of Complete Versus Incomplete Circumferential Lines Around the Pulmonary Veins During Catheter Ablation of Paroxysmal Atrial Fibrillation: Results From the Gap-Atrial Fibrillation-German Atrial Fibrillation Competence Network 1 Trial. *Circ Arrhythm Electrophysiol* 2016; 9: e003337.
5. Nanthakumar K, Plumb VJ, Epstein AE, Veenhuyzen GD, Link D, Kay GN. Resumption of electrical conduction in previously isolated pulmonary veins: rationale for a different strategy? *Circulation* 2004; 109: 1226–1229.
6. Hussein A, Das M, Riva S, et al. Use of Ablation Index-Guided Ablation Results in High Rates of Durable Pulmonary Vein Isolation and Freedom From Arrhythmia in Persistent Atrial Fibrillation Patients. *Circ Arrhythm Electrophysiol* 2018; 11: e006576.
7. Hutchinson MD, Garcia FC, Mandel JE, et al. Efforts to enhance catheter stability improve atrial fibrillation ablation outcome. *Heart Rhythm* 2013; 10: 347–353.
8. Park CI, Lehrmann H, Keyl C, et al. Mechanisms of pulmonary vein reconnection after radiofrequency ablation of atrial fibrillation: the deterministic role of contact force and interlesion distance. *J Cardiovasc Electrophysiol* 2014; 25: 701–708.

- 413 9. Piorkowski C, Eitel C, Rolf S, et al. Steerable versus non steerable sheath technology  
414 in atrial fibrillation ablation: a prospective, randomized study. *Circ Arrhythm*  
415 *Electrophysiol* 2011; 4: 157–165.
- 416 10. Chen S, Meng W, Sheng He D, et al. Blocking the pulmonary vein to left atrium  
417 conduction in addition to the entrance block enhances clinical efficacy in atrial  
418 fibrillation ablation. *Pacing Clin Electrophysiol* 2012; 35: 524–531.
- 419 11. Anter E, Contreras-Valdes FM, Shvilkin A, Tschabrunn CM, Josephson ME. Acute  
420 pulmonary vein reconnection is a predictor of atrial fibrillation recurrence following  
421 pulmonary vein isolation. *J Interv Card Electrophysiol* 2014; 39: 225–232.
- 422 12. Porta-Sánchez A, Magtibay K, Nayyar S, et al. Omnipolarity applied to equi-spaced  
423 electrode array for ventricular tachycardia substrate mapping. *Europace* 2019; 21: 813-  
424 821.
- 425 13. Kanamori N, Kato T, Sakagami S, et al. Optimal lesion size index to prevent  
426 conduction gap during pulmonary vein isolation. *J Cardiovasc Electrophysiol*. 2018;  
427 29 : 1616-1623.
- 428 14. Whitaker J, Fish J, Harrison J, et al. Lesion Index-Guided Ablation Facilitates  
429 Continuous, Transmural, and Durable Lesions in a Porcine Recovery Model. *Circ*  
430 *Arrhythm Electrophysiol*. 2018; 11: e005892.
- 431 15. Mattia L, Crosato M, Indiani S, et al. Prospective Evaluation of Lesion Index-Guided  
432 Pulmonary Vein Isolation Technique in Patients with Paroxysmal Atrial Fibrillation:  
433 1-year Follow-Up. *J Atr Fibrillation*. 2018; 10: 1858.
- 434 16. Lin C-Y, Te ALD, Lin Y-J, et al. High-resolution mapping of pulmonary vein  
435 potentials improved the successful pulmonary vein isolation using small electrodes and  
436 inter-electrode spacing catheter. *Int J Cardiol* 2018; 272: 90–96.
- 437 17. Anter E, Tschabrunn CM, Josephson ME. High-Resolution Mapping of Scar-Related  
438 Atrial Arrhythmias Using Smaller Electrodes With Closer Interelectrode Spacing. *Circ*  
439 *Arrhythm Electrophysiol* 2015; 8: 537–545.
- 440 18. Masuda M, Fujita M, Iida O, et al. The identification of conduction gaps after  
441 pulmonary vein isolation using a new electroanatomic mapping system. *Heart Rhythm*  
442 2017; 14: 1606–1614.
- 443 19. Tedrow UB, Stevenson WG. Recording and interpreting unipolar electrograms to  
444 guide catheter ablation. *Heart Rhythm* 2011; 8: 791–796.
- 445 20. Iso K, Watanabe I, Kogawa R, et al. Wavefront direction and cycle length affect left  
446 atrial electrogram amplitude. *J Arrhythm* 2017; 33: 269–274.
- 447 21. Garcia-Bolao I, Ballesteros G, Ramos B, et al. Identification of pulmonary vein  
448 reconnection gaps with high-density mapping in redo atrial fibrillation procedures.  
449 *Europace* 2018; 20: f351-f358.

450 22. McGarry TJ, Narayan SM. The Anatomical Basis of Pulmonary Vein Reconnection  
451 After Ablation for Atrial Fibrillation: Wounds That Never Felt a Scar? J Am Coll  
452 Cardiol 2012; 59: 939–941.

453 23. Kowalski M, Grimes MM, Perez FJ, et al. Histopathologic Characterization of Chronic  
454 Radiofrequency Ablation Lesions for Pulmonary Vein Isolation. J Am Coll Cardiol  
455 2012; 59: 930–938.

456

457

458

459

460

461

462

463

464

465

466

467

468

469

470

471

472

473

474

475

476



477

478 **Table 1.** Baseline characteristics of the study population

479

Number of patients	36
Gender female N (%)	14 (39)
Age (years)	66.3±8.1
CHADSVASC	2±1.2
Hypertension N (%)	11 (30.6)
Diabetes mellitus N (%)	2 (5.6)
Ischemic heart disease N (%)	1 (2.8)
Implantable device N (%)	4 (11.1)
Previous ablation N (%)	33 (91.6)
Type of procedure (de novo PAF/re-do PAF/re-do Pers, re-do AT) N (%)	3 (8.3)/ 17 (47.2)/ 11 (30.5)/ 5 (14)
LVEF (%)	53.0±11.0
LA diameter (cm)	4.10±0.60
Stroke/TIA N (%)	0 (0)
Follow-up (median months)	10 (3-24)
Free of AF N (%)	24 (83)
Complications (tamponade) N (%)	2 (5.6)

480 Values are presented as mean±SD or median (minimum-maximum).

481 Abbreviations. TIA: transient ischemic attack; LVEF: left ventricular ejection fraction; AF:

482 atrial fibrillation; PAF: paroxysmal AF; Pers: persistent; AT: atrial tachycardia

483

484

485

486

487

488

489

490

491

492

493

494

495

496 **Table 2.** Procedural characteristics

	<b>HDW</b>	<b>SB</b>	
<b>Veins with sleeves</b>	LU: 39 LL: 30 RU: 39 RL: 31	LU: 38 LL: 29 RU: 35 RL: 21	
<b>Points collected</b>	13299.6±1362.8	6952.8±841.9	p<0.001
<b>Points used</b>	2337.3±158.0	1727.5±163.8	p<0.001
<b>Sleeves Left Veins</b>	1.92±0.22	1.86±0.21	p=0.623
<b>Sleeves Right Veins</b>	1.94±0.19	1.56±0.16	p=0.018
<b>Sleeves size Left Veins</b>	40.7±5.02	37.3±5.25	p<0.001
<b>Sleeves size Right Veins</b>	49.3±6.51	34.3±4.99	p=0.024

497 Values are presented as mean±SD.

498 Abbreviations: LU: left upper; LL: left lower; RU: right upper; RL: right lower; SB: standard  
499 bipolar, HDW: High-density wave

500

501

502

503

504

505

506

507

508

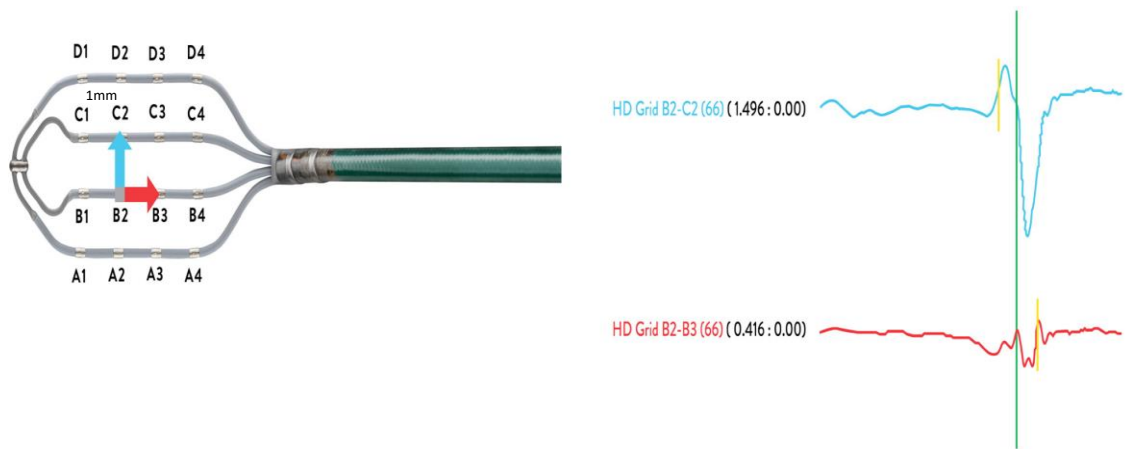
509

510

511

512

513 **Figure 1**



514  
515  
516  
517  
518  
519  
520  
521  
522  
523  
524  
525  
526  
527  
528  
529

530 **Figure 2**



531

532

533

534

535

536

537

538

539

540

541

542

543

544

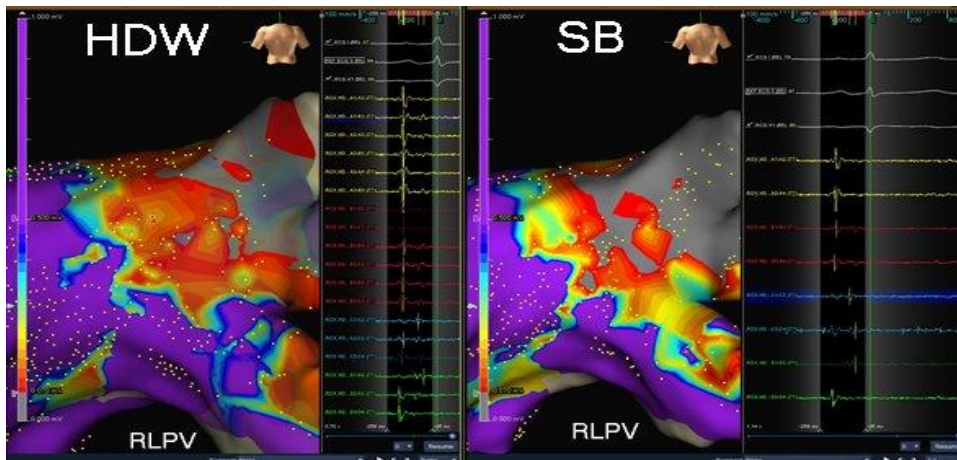
545

546

547

548 **Figure 3**

549 a)

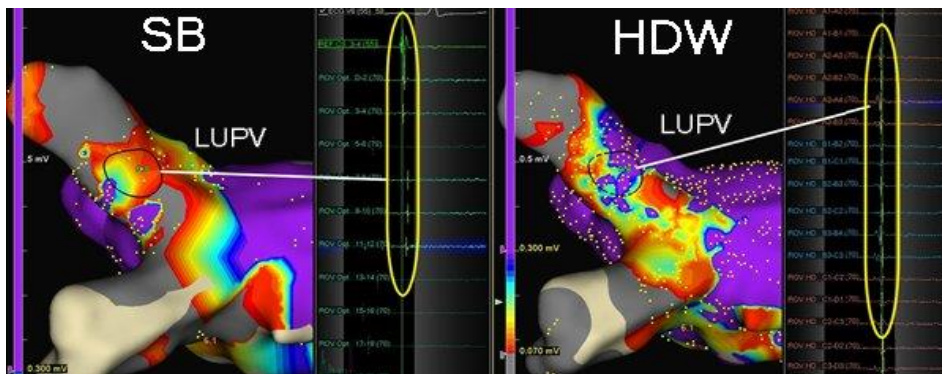


550

551

552

b)

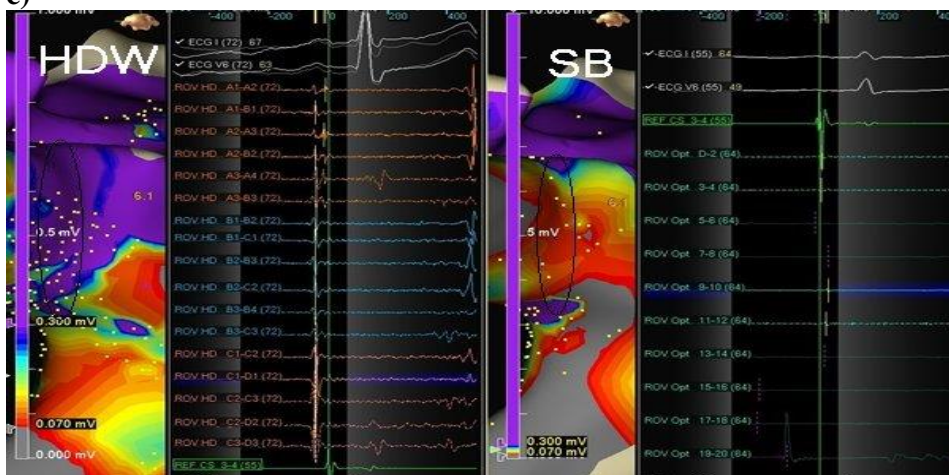


553

554

555

c)



556

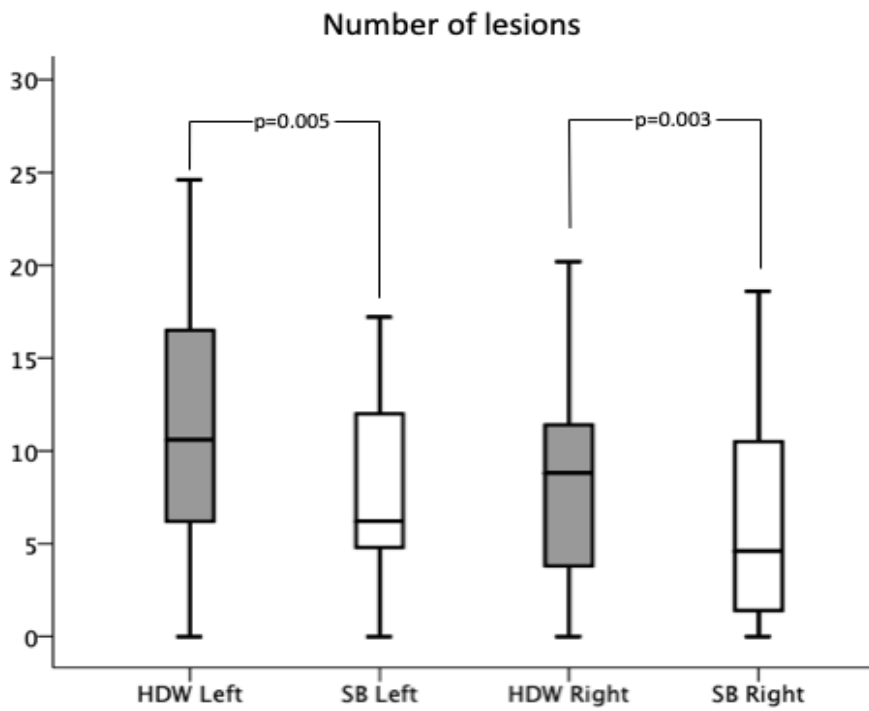
557

558

559

560 **Figure 4.** Difference in the number of lesions in left and right veins with the use of HD wave  
561 (HDW) and standard bipolar (SB)  
562

563



564

565

566

567

568

569

570

571

572

573

574

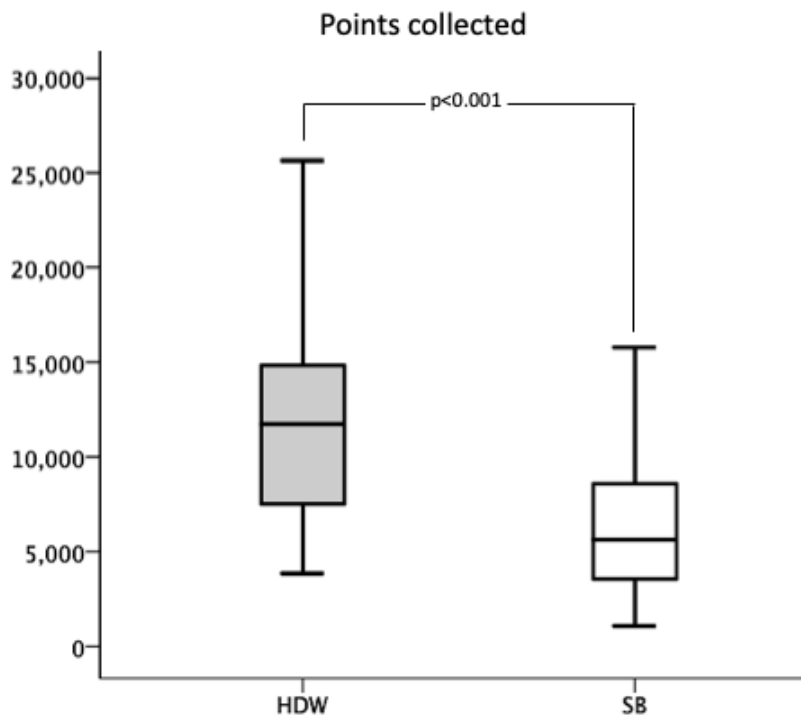
575

576

577

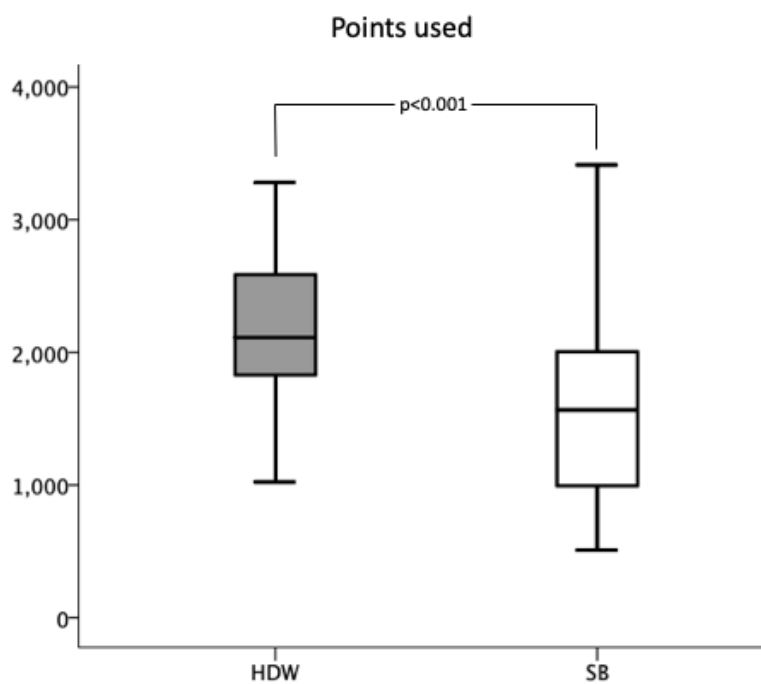
578 **Figure S1.** Difference in the number of points a) collected and b) used with HD wave  
579 (HDW) and standard bipolar (SB)  
580

581 a)



582

583 b)



584

585  
586  
587  
588  
589  
590  
591  
592  
593  
594  
595  
596  
597  
598  
599  
600  
601  
602  
603  
604  
605  
606  
607  
608  
609  
610



611

612